0273-2289/99/81/0161/$14.75

Analyte-Receptor Binding Kinetics for Different Types of Biosensors

A Fractal Analysis

ANAND RAMAKRISHNAN[1] AND AJIT SADANA*[,1,2]

[1]Chemical Engineering Department, 230 Anderson Hall, University of Mississippi, University, MS 38677-9740; and [2]Cardiology Branch, Room 7B15, Building 10, National Heart, Lung, and Blood Institute, National Institutes of Health, 10 Center Drive, MSC 1650, Bethesda, MD 20892-1650, E-mail: cmsadana@demiss.edu

Received March 29, 1999; Revised July 26, 1999; Accepted July 30, 1999

Abstract

A fractal analysis is presented for analyte-receptor binding kinetics for different types of biosensor applications. Data taken from the literature may be modeled using a single-fractal analysis, a single- and a dual-fractal analysis, or a dual-fractal analysis. The latter two methods represent a change in the binding mechanism as the reaction progresses on the surface. Predictive relationships developed for the binding rate coefficient as a function of the analyte concentration are of particular value since they provide a means by which the binding rate coefficients may be manipulated. Relationships are presented for the binding rate coefficients as a function of the fractal dimension D_f or the degree of heterogeneity that exists on the surface. When analyte-receptor binding is involved, an increase in the heterogeneity on the surface (increase in D_f) leads to an increase in the binding rate coefficient. It is suggested that an increase in the degree of heterogeneity on the surface leads to an increase in the turbulence on the surface owing to the irregularities on the surface. This turbulence promotes mixing, minimizes diffusional limitations, and leads subsequently to an increase in the binding rate coefficient. The binding rate coefficient is rather sensitive to the degree of heterogeneity, D_f, that exists on the biosensor surface. For example, the order of dependence on D_{f1} is 7.25 for the binding rate coefficient k_1 for the binding of a Fab fragment of an antiparaquat monoclonal antibody in solution to an antigen in the form of a paraquat analog immobilized on a sensor surface. The predictive relationships presented for the binding rate coefficient and the fractal dimension as a function of the analyte concentration in solution provide further physical insights into the binding reactions on the surface, and should assist in

*Author to whom all correspondence and reprint requests should be addressed.

enhancing biosensor performance. In general, the technique is applicable to other reactions occurring on different types of surfaces, such as cell-surface reactions.

Index Entries: Analyte-receptor binding; fractals; biosensors.

Introduction

Sensitive detection systems (or sensors) are required to distinguish a wide range of substances. Sensors find application in the areas of biotechnology, physics, chemistry, medicine, aviation, oceanography, and environmental control. These sensors or biosensors may be utilized to monitor the analyte-receptor reactions in real time *(1)*. The importance of providing a better understanding of the mode of operation of biosensors to improve their sensitivity, stability, and specificity has been emphasized *(2)*. A particular advantage of this method is that no reactant labeling is required. However, for the binding interaction to occur, one of the components has to be bound or immobilized onto a solid surface. This often leads to mass-transfer limitations and subsequent complexities. Nevertheless, the solid-phase immunoassay technique represents a convenient method for the separation and/or detection of reactants (e.g., antigen) in a solution since the binding of antigen to an antibody-coated surface (or vice versa) is sensed directly and rapidly. There is a need to characterize the reactions occurring at the biosensor surface in the presence of diffusional limitations that are inevitably present in these types of systems.

The details of the association of analyte (antibody or substrate) to a receptor (antigen or enzyme) immobilized on a surface is of tremendous significance for the development of immunodiagnostic devices as well as for biosensors *(3)*. In essence, the analysis to be presented is, in general, applicable to ligand-receptor and analyte-receptorless systems for biosensor and other applications (e.g., membrane-surface reactions). External diffusional limitations play a role in the analysis of immunodiagnostic assays *(4–9)*. The influence of diffusion in such systems has been analyzed to some extent *(6,10–18)*. The influence of partial *(19)* and total *(20–22)* mass transport limitations on analyte-receptor binding kinetics for biosensor applications is available. The analysis presented for partial mass transport limitation *(19)* is applicable to simple one-to-one association as well as cases in which there is heterogeneity of the analyte or the ligand. This applies to the different types of biosensors utilized for the detection of different analytes.

Chiu and Christpoulos *(23)* emphasize that the strong and specific interaction of two complementary nucleic acid strands is the basis of hybridization assays. Syvanen et al. *(24)* have analyzed the hybridization of nucleic acids by affinity-based hybrid collection. In their method, a probe pair is allowed to form hybrids with the nucleic acid in solution. They emphasize that their procedure is quantitative and has a detection limit of 0.67 attamoles. Bier et al. *(25)* have recently analyzed the reversible binding

of DNA oligonucleotides in solution to immobilized DNA targets using a grating coupler detector and surface plasmon resonance. These investigators emphasize that the major fields of interest for hybridization analysis are clinical diagnostics and hygiene. The performance of these "genosensors" will be significantly enhanced when more physical insights are obtained for each of the procedures or steps that are involved in the entire assay.

An optical technique that has gained increasing importance in recent years is the surface plasmon resonance (SPR) technique *(26)*. This is particularly so owing to the development and availability of the BIAcore (BIAcore AB, Uppsala, Sweden) biosensor, which is based on the SPR method and has found increasing industrial usage. Bowles et al. *(27)* have recently used the BIAcore biosensor to analyze the binding kinetics of Fab fragments of an antiparaquat antibody in solution to a paraquat analog (antigen) covalently attached at a sensor surface. Schmitt et al. *(28)* have also utilized a modified form of the BIAcore biosensor to analyze the binding of thrombin in solution to antithrombin covalently attached to a sensor surface. The performance of SPR and other biosensors will be enhanced when more physical insights are obtained for each of these analytical procedures.

Kopelman *(29)* indicates that surface diffusion-controlled reactions that occur on clusters or islands are expected to exhibit anomalous and fractal-like kinetics. These fractal kinetics exhibit anomalous reaction orders and time-dependent rate (e.g., binding) coefficients. Fractals are disordered systems with the disorder described by nonintegral dimensions *(30)*. Kopelman *(29)* further indicates that as long as surface irregularities show scale invariance that is dilatational symmetry, they can be characterized by a single number, the fractal dimension. The fractal dimension is a global property and is insensitive to structural or morphological details *(31)*. Markel et al. *(32)* indicate that fractals are scale, self-similar mathematical objects that possess nontrivial geometrical properties. Furthermore, these investigators indicate that rough surfaces, disordered layers on surfaces, and porous objects all possess fractal structure. A consequence of the fractal nature is a power-law dependence of a correlation function (in our case analyte-receptor complex on the surface) on a coordinate (e.g., time).

Antibodies are heterogeneous and their immobilization on a fiber-optic surface, e.g., would exhibit some degree of heterogeneity. This is a good example of a "disordered system," and a fractal analysis is appropriate for such systems. In addition, the antibody-antigen reaction on the surface is a good example of a low-dimension reaction system in which the distribution tends to be "less random" *(29)*. A fractal analysis would provide novel physical insights into the diffusion-controlled reactions occurring at the surface. Markel et al. *(32)* indicate that fractals are widespread in nature. Dendrimers are a class of polymers with internal voids and possess unique properties. The stepwise buildup of six internal dendrimers into a dendrimer exhibits typical fractal (self-similar) characteristics *(33)*. Fractal kinetics have been reported in biochemical reactions such as the

gating of ion channels *(34,35)*, enzyme reactions *(36)*, and protein dynamics *(37)*. It has been emphasized that the nonintegral dimensions of the Hill coefficient used to describe the allosteric effects of proteins and enzymes is a direct consequence of the fractal property of proteins *(36)*.

Strong fluctuations in fractals have not been taken into account *(32)*. For example, strongly fluctuating fields greatly enhance Raman scattering from fractals. It would be of interest to determine a fractal dimension for biosensor applications and to determine whether there is a change in the fractal dimension as the binding reaction proceeds on the biosensor surface, the final goal being how this affects the binding rate coefficient and subsequently biosensor performance. Fractal aggregate scaling relationships have been determined for both diffusion-limited and diffusion-limited scaling aggregation processes in spatial dimensions 2, 3, 4, and 5 *(38)*. Fractal dimension values for the kinetics of antigen-antibody binding *(39,40)* and analyte-receptor *(41)* binding for fiber-optic biosensor systems are available. In these studies the influence of the experimental parameters such as analyte concentration on the fractal dimension and on the binding rate coefficient (the "prefactor" in this case) were analyzed.

One would like to delineate the role of surface roughness on the speed of response, specificity, stability, and sensitivity of fiber-optic and other biosensors. An initial attempt has been made to relate the influence of surface roughness (or fractal dimension) on the binding rate coefficient for fiber-optic and other biosensors *(42)*. High and fractional orders of dependence of the binding rate coefficient on the fractal dimension were obtained. We now extend these studies to more biosensor applications, including those in which more than one fractal dimension is involved at the biosensor surface—in other words, in which complex binding mechanisms, as well as a change in the binding mechanism may be involved at the surface. Quantitative relationships for the binding rate coefficient as a function of the fractal dimension are obtained for different biosensor applications. The noninteger orders of dependence obtained for the binding rate coefficient on the fractal dimension further reinforce the fractal nature of these analyte-receptor binding systems.

Theory

An analysis of the binding kinetics of antigen in solution to antibody immobilized on the biosensor surface is available *(40)*. The influence of lateral interactions on the surface and variable rate coefficients is also available *(43)*. Here, we initially present a method of estimating actual fractal dimension values for analyte-receptor binding systems utilized in fiber-optic biosensors.

Variable Binding Rate Coefficient

Kopelman *(29)* has indicated that classical reaction kinetics is sometimes unsatisfactory when the reactants are spatially constrained on the

microscopic level by walls, phase boundaries, or force fields. Such heterogeneous reactions, e.g., bioenzymatic reactions, that occur at interfaces of different phases exhibit fractal orders for elementary reactions and rate coefficients with temporal memories. In such reactions, the rate coefficient exhibits a form given by

$$k_1 = k' t^{-b} \tag{1}$$

In general, k_1 depends on time, whereas, $k' = k_1(t = 1)$ does not. Kopelman *(29)* indicates that in three dimensions (homogeneous space), $b = 0$. This is in agreement with the results obtained in classical kinetics. Also, with vigorous stirring, the system is made homogeneous and b again equals 0. However, for diffusion-limited reactions occurring in fractal spaces, $b > 0$; this yields a time-dependent rate coefficient.

The random fluctuations in a two-state process in ligand binding kinetics has been analyzed *(44)*. The stochastic approach can be used as a means to explain the variable binding rate coefficient. The simplest way to model these fluctuations is to assume that the binding rate coefficient $k_1(t)$ is the sum of its deterministic value (invariant) and the fluctuation (z[t]) *(44)*. This $z(t)$ is a random function with a zero mean. The decreasing and increasing binding rate coefficients can be assumed to exhibit an exponential form *(45)*.

Sadana and Madagula *(43)* analyzed the influence of a decreasing and an increasing binding rate coefficient on the antigen concentration when the antibody is immobilized on the surface. These investigators noted that for an increasing binding rate coefficient, after a brief time interval, as time increases, the concentration of the antigen near the surface decreases, as expected for the cases when lateral interactions are present or absent. The diffusion-limited binding kinetics of antigen (or antibody or substrate) in solution to antibody (or antigen or enzyme) immobilized on a biosensor surface has been analyzed within a fractal framework *(39,40)*. Furthermore, experimental data presented for the binding of human immunodeficiency virus (HIV) (antigen) to the antibody anti-HIV immobilized on a surface show a characteristic ordered "disorder" *(45)*. This indicates the possibility of a fractal-like surface. It is obvious that the above biosensor system (wherein either the antigen or the antibody is attached to the surface) along with its different complexities, including heterogeneities on the surface and in solution, diffusion-coupled reactions, and time-varying adsorption or binding rate coefficients, can be characterized as a fractal system. The diffusion of reactants toward fractal surfaces has been analyzed *(46)*. Havlin *(47)* has briefly reviewed and discussed these results.

Single-Fractal Analysis

Havlin *(47)* indicates that the diffusion of a particle (antibody [Ab]) from a homogeneous solution to a solid surface (e.g., antigen [Ag]-coated surface) in which it reacts to form a product (antibody-antigen complex; Ab · Ag) is given by

$$[\text{analyte} \cdot \text{receptor}] \alpha \begin{cases} t^{(3-D_f)/2} = t^P & t < t_c \\ & \text{time, } t\text{, less than } t_c \\ t^{1/2} & t > t_c \\ & \text{time, } t\text{, greater than } t_c \end{cases} \quad (2a)$$

Here D_f is the fractal dimension of the surface. Equation 2a indicates that the concentration of the product Ab · Ag(t) in a reaction Ab + Ag → Ab · Ag on a solid fractal surface scales at short and intermediate scales as [Ab · Ag] ~ t^p with the coefficient $p = (3 - D_f)/2$ at short time scales, and $p = 1/2$ at intermediate time scales. This equation is associated with the short-term diffusional properties of a random walk on a fractal surface. Note that in a perfectly stirred kinetics on a regular (nonfractal) structure (or surface), k_1 is a constant; that is, it is independent of time. In other words, the limit of regular structures (or surfaces) and the absence of diffusion-limited kinetics leads to k_1 being independent of time. In all other situations, one would expect a scaling behavior given by $k_1 \sim k' t^{-b}$ with $-b = p < 0$. Also, the appearance of the coefficient p different from $p = 0$ is the consequence of two different phenomena, i.e., the heterogeneity (fractality) of the surface and the imperfect mixing (diffusion-limited) condition.

Havlin *(47)* indicates that the crossover value may be determined by $r_c^2 \sim t_c$. Above the characteristic length, r_c, the self-similarity is lost. Above t_c, the surface may be considered homogeneous, since the self-similarity property disappears, and "regular" diffusion is now present. For the present analysis, t_c is arbitrarily chosen. For the purpose of this analysis, we assume that the value of t_c is not reached. One may consider the analysis to be presented as an intermediate "heuristic" approach in that in the future one may also be able to develop an autonomous (and not time-dependent) model of diffusion-controlled kinetics.

Dual-Fractal Analysis

The single-fractal analysis we have just presented is extended to include two fractal dimensions. At present, the time ($t = t_1$) at which the first fractal dimension "changes" to the second fractal dimension is arbitrary and empirical. For the most part, it is dictated by the data analyzed and the experience gained by handling a single-fractal analysis. A smoother curve is obtained in the "transition" region, if care is taken to select the correct number of points for the two regions. In this case, the product (Ab · Ag) concentration on the biosensor surface is given by:

$$[\text{analyte} \cdot \text{receptor}] \alpha \begin{cases} t^{(3-D_{f_1})/2} = t^{P_1} & t < t_1 \\ & \text{time, } t\text{, less than } t_1 \\ t^{(3-D_{f_2})/2} = t^{P_2} & t_1 < t < t_2 = t_c \\ & \text{time, } t\text{, in the range between } t_1 \text{ and } t_2 \\ t^{1/2} & t > t_c \\ & \text{time, } t\text{, greater than } t_c \end{cases} \quad (2b)$$

Results

At the outset, it is appropriate to indicate that a fractal analysis will be applied to data obtained for analyte-receptor binding data with different types of biosensors. This is one possible explanation for analyzing the diffusion-limited binding kinetics assumed to be present in all of the systems analyzed. The parameters thus obtained would provide a useful comparison of different situations. Alternate expressions involving saturation, first-order reaction, and no diffusion limitations are possible, but they are apparently deficient in describing the heterogeneity that inherently exists on the surface. The analyte-receptor binding reaction on the different types of biosensors analyzed is a complex reaction, and the fractal analysis via the fractal dimension and the binding rate coefficient provide a useful lumped parameter(s) analysis of the diffusion-limited situation.

Schmitt et al. *(28)* recently analyzed the binding of thrombin in solution to antithrombin immobilized on a transducer surface using a BIAcore biosensor. They utilized reflectometric interference spectroscopy as a transducer. The antibody group was immobilized on the transducer surface with carboxymethyldextran (CMD) by diisopropylcarbodiimide (DIC) activation. The experimental data were represented in optical thickness. Schmitt et al. *(28)* indicated that an approx 1-nm change in optical thickness was observed for 1 ng of protein bound/mm^2 of transducer surface. Figure 1A shows the curves obtained using Eq. 2a for the binding of 1 μg/mL of thrombin in solution to 2 mg of antithrombin immobilized on the transducer surface. A single-fractal analysis is sufficient to describe the binding kinetics. The entire binding curve is utilized to obtain the fractal dimension and the binding rate coefficient.

Table 1 shows the values of the binding rate coefficient k and the fractal dimension D_f. The values of the binding rate coefficient(s) and the fractal dimension(s) presented in Table 1 were obtained from a regression analysis using Sigmaplot *(48)* to model the experimental data using Eq. 2a, wherein $[\text{analyte} \cdot \text{receptor}] = kt^p$. The k and D_f values presented in Table 1 are within 95% confidence limits. For example, for the binding of 1 μg/mL of thrombin in solution to 2 mg of antithrombin immobilized on the transducer surface shown in Fig. 1A, the value of k reported is 0.00072 ± 0.000069. The 95% confidence limits indicates that 95% of the k values will lie between 0.00065 and 0.00079. This indicates that the values are precise and significant. The curves presented in the figures are theoretical curves.

Figure 1B,C shows the binding of 2.0 and 5.0 μg/mL of thrombin in solution to antithrombin immobilized on a sensor surface, respectively. In both of these cases, a single-fractal analysis is sufficient to describe the binding kinetics adequately. The values of the binding rate coefficient and the fractal dimension are given in Table 1. Note that as the thrombin concentration in solution is increased from 1 to 5 μg/mL, k increases from a value of 0.00072 to 0.0048, and D_f decreases from a value of 1.06 to 0.85.

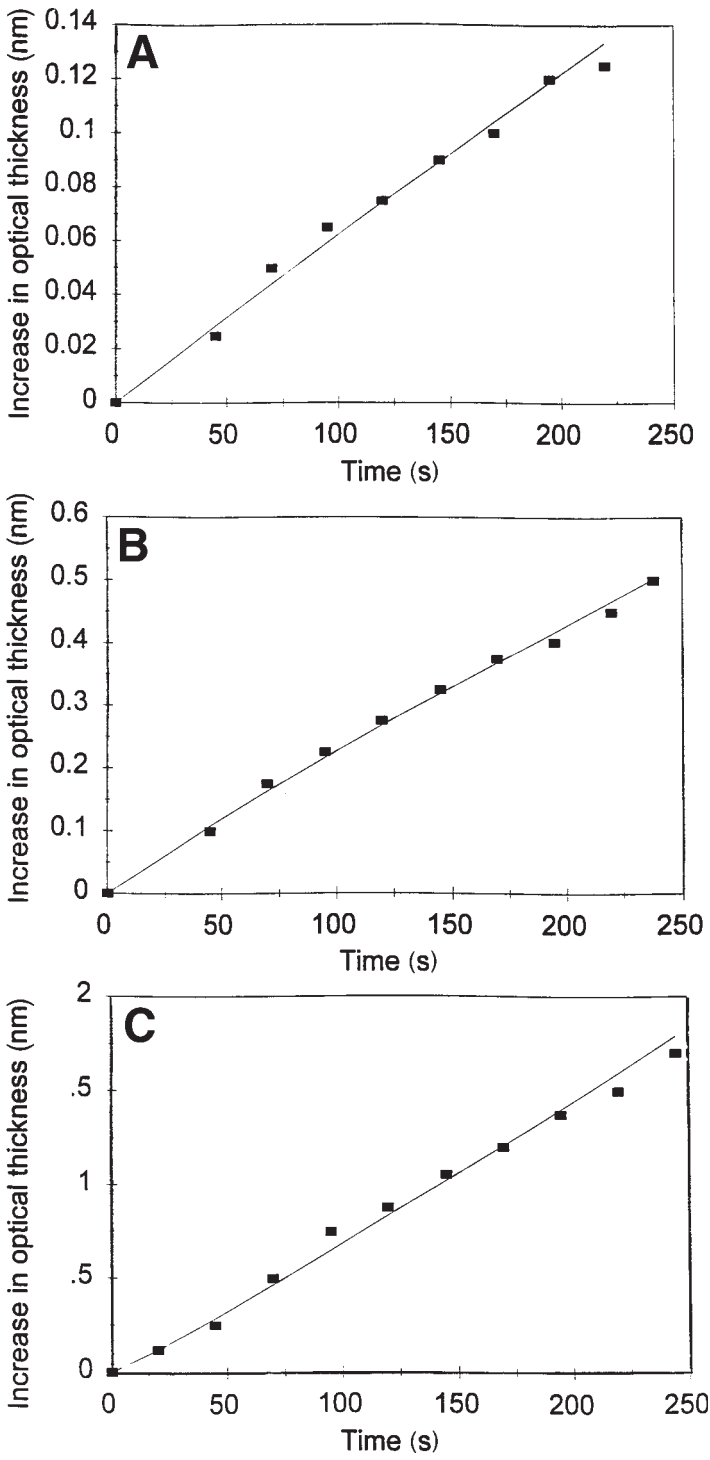

Fig. 1. Binding of different concentrations of thrombin in solution to 2 mg of antithrombin immobilized on a transducer surface *(28)*: **(A)** 1.0 µg/mL; **(B)** 2.0 µg/mL; **(C)** 5.0 µg/mL.

Table 1
Influence of Thrombin Concentration in Solution on Binding Rate Coefficients and Fractal Dimensions for Its Binding to Antithrombin Immobilized on a Transducer Surface Using a BIAcore Biosensor[a]

Thrombin concentration in solution[b]	Binding rate coefficient, k (nanometers of t^{-p}), from Eq. 2a[c]	Fractal dimension, D_f
1.0	0.00072 ± 0.000069	1.06 ± 0.13
2.0	0.0033 ± 0.0007	1.16 ± 0.06
5.0	0.0048 ± 0.0004	0.85 ± 0.07

[a]Reproduced with permission from ref. *28*.
[b]Given as (μg/mL)/2 mg antithrombin immobilized on transducer surface modified with CMD by DIC activation.
[c]One nanometer in optical thickness is approximately equal to 1 ng of protein bound/mm^2 of transducer surface.

There is no nonselective adsorption of the thrombin. Our analysis, at present, does not include this nonselective adsorption. We do recognize that, in some cases, this may be a significant component of the adsorbed material and that this rate of association, which is of a temporal nature, would depend on surface availability. If we were to accommodate the nonselective adsorption into the model, there would be an increase in the degree of heterogeneity on the surface, since by its very nature nonspecific adsorption is more heterogeneous than specific adsorption. This would lead to higher fractal dimension values since the fractal dimension is a direct measure of the degree of heterogeneity that exists on the surface. Future analysis of analyte-receptor binding data may include this aspect in the analysis, which would be exacerbated by the presence of inherent external diffusional limitations.

Furthermore, we do not present any independent proof or physical evidence for the existence of fractals in the analysis of these analyte-receptor binding systems except by indicating that it has been applied in other areas and that it is a convenient means to make more quantitative the degree of heterogeneity that exists on the surface. Thus, in all fairness, this is one possible way by which to analyze this analyte-receptor binding data. One might justifiably argue that appropriate modeling may be achieved by using a Langmuirian or other approach. The Langmuirian approach has a major drawback because it does not allow for or accommodate the heterogeneity that exists on the surface.

Table 1 indicates that k increases as the thrombin concentration in solution increases. Figure 2A shows an increase in k with an increase in the thrombin concentration in solution. Clearly, k varies with thrombin concentration in a nonlinear fashion. In the thrombin concentration range (1–5 μg/mL) analyzed, k is given by

$$k = (0.00094 \pm 0.00072)\ [\text{thrombin}]^{1.14 \pm 0.50} \quad (3a)$$

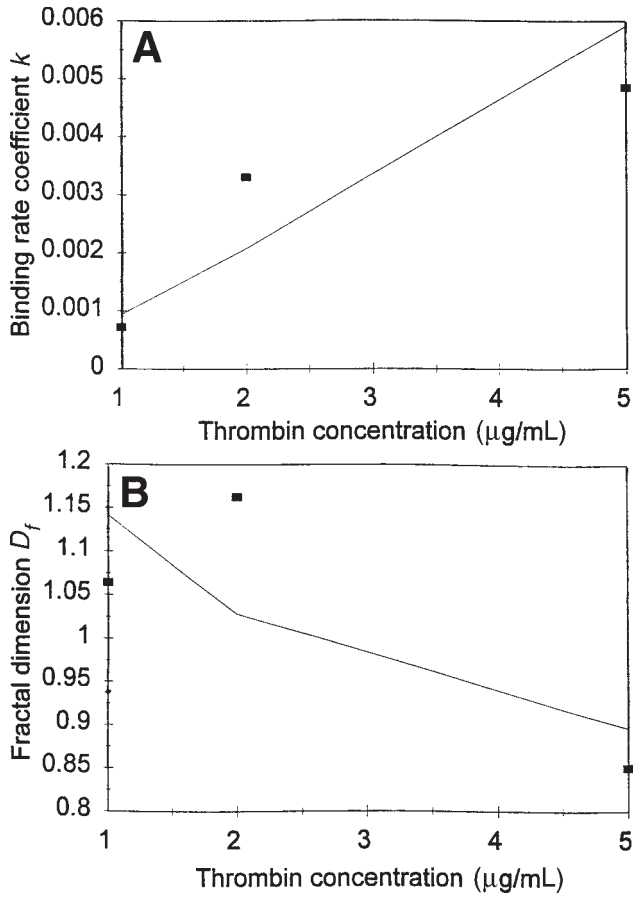

Fig. 2. Influence of the thrombin concentration (micrograms/milliliter) in solution on **(A)** the binding rate coefficient *k*; and **(B)** the fractal dimension D_f.

There is scatter in the data, and this is clearly indicated in the error estimates of the values of the exponent and the constant. More data points are required to establish this equation more firmly. Nevertheless, Eq. 3a is of value since it provides an indication of the change in *k* as the thrombin concentration in solution changes.

Table 1 indicates that D_f decreases as the thrombin concentration in solution increases. Figure 2B shows the decrease in D_f with an increase in the thrombin concentration in solution. In the thrombin concentration range (1–5 μg/mL) analyzed, the D_f is given by

$$D_f = (1.14 \pm 0.19)\ [\text{thrombin}]^{-0.15 \pm 0.13} \quad (3b)$$

There is scatter in the data, and this is clearly indicated in the value of the exponent. More data points would more firmly establish this relation. Nevertheless, Eq. 3a is valuable because it provides an indication of the change in D_f as the thrombin concentration in solution changes. One may wish to substitute Eq. 3b for thrombin concentration in terms of D_f in Eq. 3a

in order to obtain an expression for k in terms of D_f. Since these are already secondary equations in themselves, it is perhaps not appropriate to perform this substitution and obtain an expression for k in terms of D_f. If one were to do this, an order of dependence of k on D_f of –9.32 would be obtained.

Su et al. *(49)* recently analyzed the hybridization kinetics of interfacial RNA homopolymer using a thickness-shear mode acoustic wave biosensor. These investigators indicate that the binding or hybridization mechanism involves the diffusion of the RNA probe molecules in solution followed by duplex formation at the surface. They attempted to analyze the influence of temperature, buffer solutions, and blocking agents on the hybridization kinetics.

Figure 3A shows the binding of RNA homopolymer in solution to polycytidylic acid (5') (poly C) immobilized on an electrode surface. The rough electrode surface was treated with Denhardt's reagent (stock solution containing 10 g of Ficoll, 10 g of polyvinylpyrrolidone, and 10 g of bovine serum albumin in 500 mL of water); this was run no. 2 carried out at 24°C (*see* Table 2). A single fractal analysis is sufficient to describe the binding kinetics adequately. A single-fractal analysis underestimates the data at medium times and overestimates the data at longer times. Since the error estimate for k was small compared to the value estimated (8.66 ± 0.59), a dual-fractal analysis was not utilized. This was the case for the D_f value as well. Surely, a dual-fractal analysis has more parameters and it would provide a better fit. In addition, the data may fit a Langmuir isotherm. However, this Langmuir isotherm has a major drawback, in that it cannot accommodate for the heterogeneity that exists on the surface.

Figure 3B shows the binding of RNA homopolymer in solution to poly C immobilized on an electrode surface. In this case the rough electrode surface was untreated; this was run no. 1. In this case, a dual-fractal analysis is required to describe the binding kinetics adequately. Table 2 gives the values of k and D_f for a single-fractal analysis, and the binding rate coefficients k_1 and k_2 and the fractal dimensions D_{f1} and D_{f2} for a dual-fractal analysis.

Figure 3C shows the binding of RNA homopolymer in solution to poly C immobilized on an electrode surface. In this case the rough electrode surface was treated with Denhardt's reagent and ss salmon test DNA together; this was run no. 3 carried out at 24°C (*see* Table 2). Once again, a dual-fractal analysis is required to describe the binding kinetics adequately. Interestingly, when one goes from a single- to a dual-fractal analysis to describe the binding curves, an inherent change in the binding mechanism takes place. For example, consider the curves presented in Fig. 3A–C. Figure 3A requires a single-fractal analysis to describe the binding curve, whereas in Fig. 3B,C a dual-fractal analysis is required to describe the binding curve.

Figure 3D shows the binding of RNA homopolymer in solution to poly C immobilized on an electrode surface. In this case 5X SSC (NaCl and sodium citrate) hybridization buffer solution was used; this was run no. 4 carried out at 24°C (*see* Table 2). A dual-fractal analysis is required to

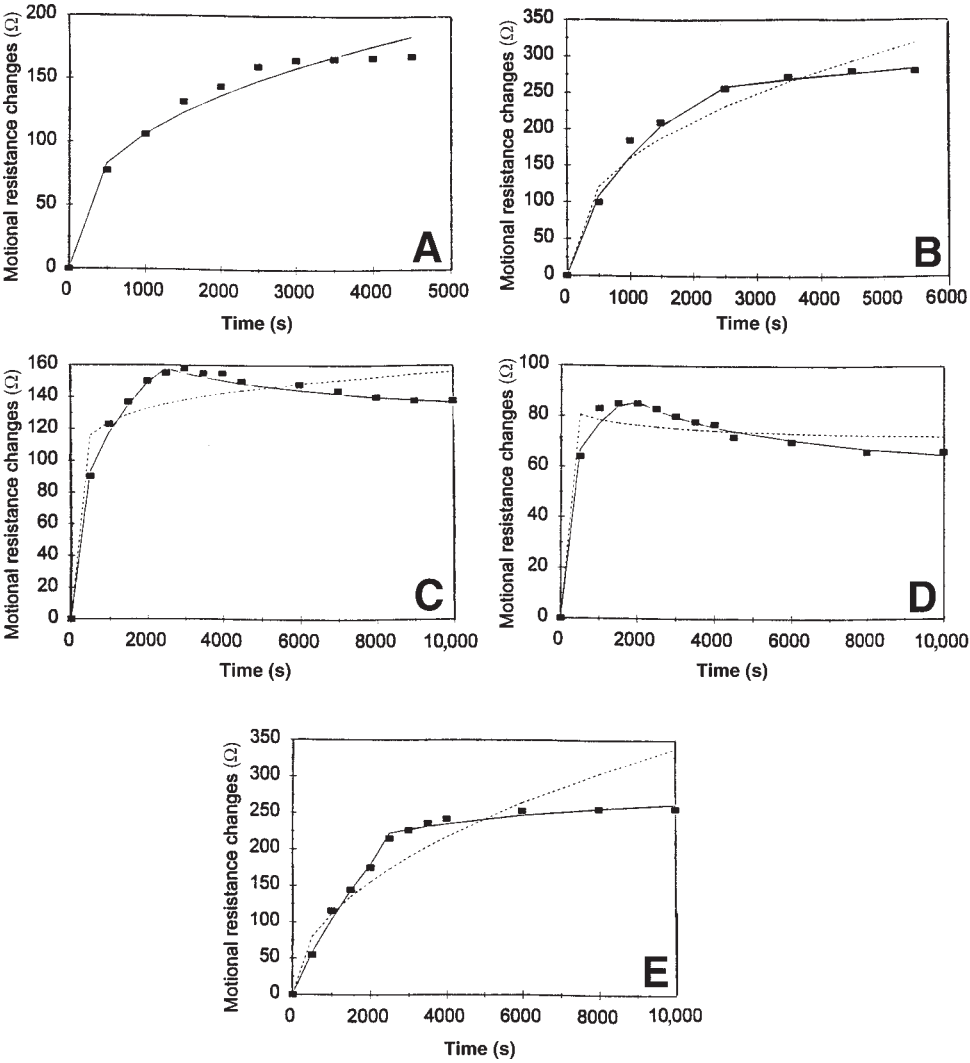

Fig. 3. RNA homopolymerization on an electrode-solution surface *(49)*: **(A)** run no. 2; **(B)** run no. 1; **(C)** run no. 3; **(D)** run no. 4; **(E)** run no. 5. (- - - -), Single-fractal analysis; (——), dual-fractal analysis.

describe the binding kinetics adequately. Figure 3E shows the binding of RNA homopolymer in solution to poly C immobilized on an electrode surface. In this case the electrode surface was smooth; this was run no. 5 (*see* Table 2). Once again, a dual-fractal analysis is required to describe the binding kinetics adequately.

It is of interest to compare the results presented in Fig. 3B and Fig. 3E, in which a dual-fractal analysis was utilized to describe the binding kinetics. Both electrode surfaces were untreated. In run no. 1 a rough electrode surface was utilized, and in run no. 5 a smooth electrode surface was utilized. One might anticipate that the fractal dimension in run no. 1 should

Table 2
Influence of Different Conditions
on the Fractal Dimensions and Binding Rate Coefficients
for RNA Homopolymer Hybridization on an Electrode-Solution Interface[a]

Run number	k	D_f	k_1	k_2	D_{f1}	D_{f2}
1	8.66 ± 0.59	2.27 ± 0.06	NA	NA	NA	NA
2	9.87 ± 1.49	2.19 ± 0.13	2.99 ± 0.39	102.46 ± 1.63	1.84 ± 0.21	2.76 ± 0.05
3	62.34 ± 7.92	2.80 ± 0.07	11.19 ± 0.44	358.82 ± 5.52	2.32 ± 0.06	3.0 – 0.02
4	101.81 ± 11.28	3.0 – 0.07	18.04 ± 1.29	322.69 ± 5.76	2.58 ± 0.13	3.0 – 0.02
5	3.98 ± 0.89	2.03 ± 0.14	0.36 ± 0.03	87.54 ± 2.37	1.36 ± 0.13	2.76 ± 0.04

[a]Reproduced with permission from ref. *49*. NA, not applicable.

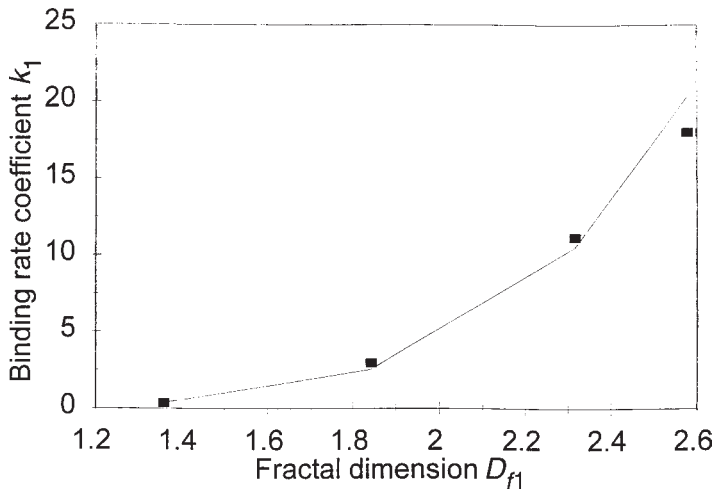

Fig. 4. Influence of the fractal dimension D_{f1} on the binding rate coefficient k_1.

be higher than that observed in run no. 5. This should be true at time, t, close to zero, which correctly describes the nature of the surface, and which has not been influenced by the reaction occurring at the surface. Table 2 indicates that, as expected, the fractal dimension for run no. 1 (D_{f1} = 1.84) is higher than that observed for run no. 5 (D_{f1} = 1.36). The second fractal dimensions, D_{f2}, obtained for runs no. 1 (=2.764) and no. 5 (2.762) are very close to each other. In this case the surface has now been made complex thanks to the reaction taking place on the surface. Besides, the maximum value that the fractal dimension can have is 3. Thus, no comments are made with regard to a comparison of the D_{f2} values observed.

Finally, on examining the values of D_{f1} and k_1 obtained in Table 2, one notes that an increase in the fractal dimension leads to an increase in the binding rate coefficient k_1. This can be seen in Fig. 4. For run nos. 1, 3, 4, and 5, in which a dual-fractal analysis is applicable, the binding rate coefficient k_1 is given by

$$k_1 = (0.059 \pm 0.010) D_{f1}^{6.17 \pm 0.32} \quad (4)$$

Bowles et al. *(27)* recently analyzed the binding of a Fab fragment of an antiparaquat monoclonal antibody in solution and an immobilized antigen in the form of a paraquat analog immobilized on a sensor surface. One of the aims of their study was to develop a method to obtain kinetic constants from data (sensorgrams) that exhibited other than first-order behavior, or deviated from pseudo-first-order behavior. Figure 5A shows the binding of a 4 μ*M* Fab fragment of an antiparaquat antibody in solution to an antigen (paraquat analog) immobilized on a sensor chip. A dual-fractal analysis is required to adequately describe the binding kinetics adequately (*see* Table 2). One might argue that the data in Fig. 5A appear to follow a Langmuirian isotherm. As indicated previously, the Langmuirian isotherm does not accommodate for the heterogeneity that exists on the surface. The saturated response in Fig. 5A is represented in our analysis with a fractal dimension of 2.87. This indicates a very high level of heterogeneity on the surface. This value of 2.87 is close to the maximum value of 3.0.

Figure 5B shows the binding of a 1.25 μ*M* Fab fragment of an antiparaquat antibody in solution to paraquat (analog) sites immobilized on a sensor chip. In this case too, a dual-fractal analysis is required to describe the binding kinetics adequately (*see* Table 2). Figure 5C shows the binding of a 10 μ*M* Fab fragment of an antiparaquat antibody in solution to paraquat (analog) sites immobilized on a sensor chip. Once again, a dual-fractal analysis is required to describe the binding kinetics adequately (*see* Table 2). Interestingly, an increase in the Fab fragment concentration in solution by a factor of 8 from 1.25 to 10 μ*M* leads to increases in k_1 and k_2 and in D_{f1} and D_{f2}. For example, k_1 increases by a factor of 11.85 from a value of 650.4 to 7705.9.

For the three runs presented in Table 3, one notes that an increase in the fractal dimension D_{f1} leads to an increase in the binding rate coefficient k_1. For these runs, k_1 is given by

$$k_1 = (13.15 \pm 10.60) D_{f1}^{7.25 \pm 1.65} \quad (5)$$

Figure 6 shows that Eq. 5 fits the data reasonably well. There is some deviation in the estimated value of the exponent in spite of the fact that the fit is quite reasonable. Only three data points are available; more data points would more firmly establish this relationship. The binding rate coefficient is very sensitive to the degree of heterogeneity on the surface, as can be noted by the very high value of the exponent. The fractional order of dependence further reinforces the fractal nature of the system.

Note that an increase in the degree of heterogeneity on the surface leads to an increase in the binding rate coefficient. One possible explanation for this effect is that because of the rough surfaces, additional interactions arise; for example, turbulent flow is generated by the protruding surfaces and fluid is entrapped in small "holes" on the surface *(50)*. This turbulence would enhance the localized mixing, which would lead to a decrease in the

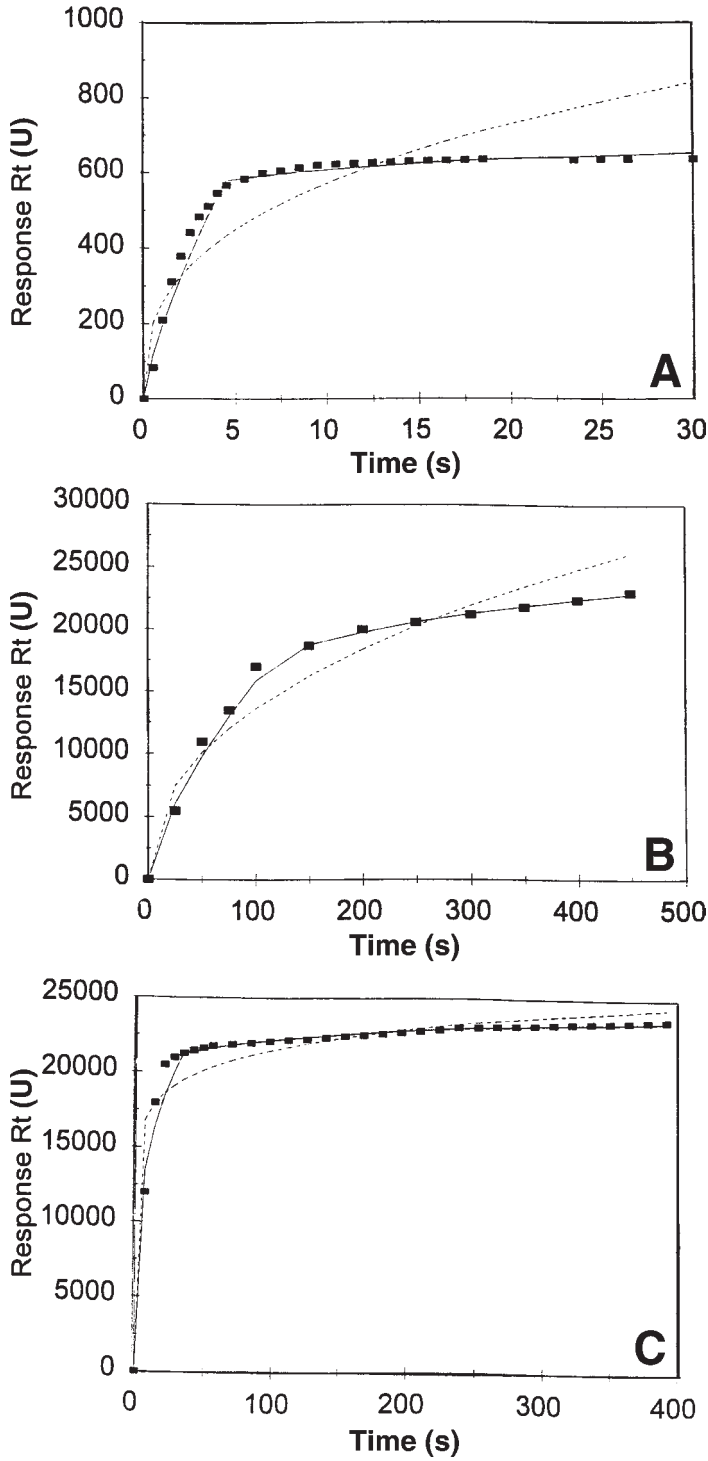

Fig. 5. Binding of the Fab fragment of an antiparaquat antibody in solution to a paraquat analog immobilized on a sensor chip *(27)*: **(A)** 4 µ*M*; **(B)** 1.25 µ*M*; **(C)** 10 µ*M*. (- - - -), Single-fractal analysis; (——), dual-fractal analysis.

Table 3
Fractal Dimensions and Binding Rate Coefficients for the Binding of Fab Fragment of an Antiparaquat Antibody in Solution to Paraquat Analog Immobilized on a Sensor Chip[a]

Fab fragment in solution/ receptor on surface	k	D_f	k_1	k_2	D_{f1}	D_{f2}
4 μ*M* Fab fragment of an antiparaquat antibody/paraquat analog immobilized on sensor chip	256.52 ± 72.64	2.30 ± 0.09	193.78 ± 38.26	527.55 ± 10.38	1.53 ± 0.15	2.87 ± 0.02
1.25 μ*M* Fab fragment of an antiparaquat antibody/paraquat analog immobilized on sensor chip	1867.78 ± 319.43	2.14 ± 0.11	650.42 ± 82.27	7623.69 ± 46.90	1.61 ± 0.17	2.64 ± 0.10
10 μ*M* Fab fragment of an antiparaquat antibody/paraquat analog immobilized on sensor chip	14,074.87 ± 1097.87	2.82 ± 0.03	7705.94 ± 757.34	18,275.05 ± 75.08	2.43 ± 0.11	2.92 ± 0.00

[a]Reproduced with permission from ref. 27.

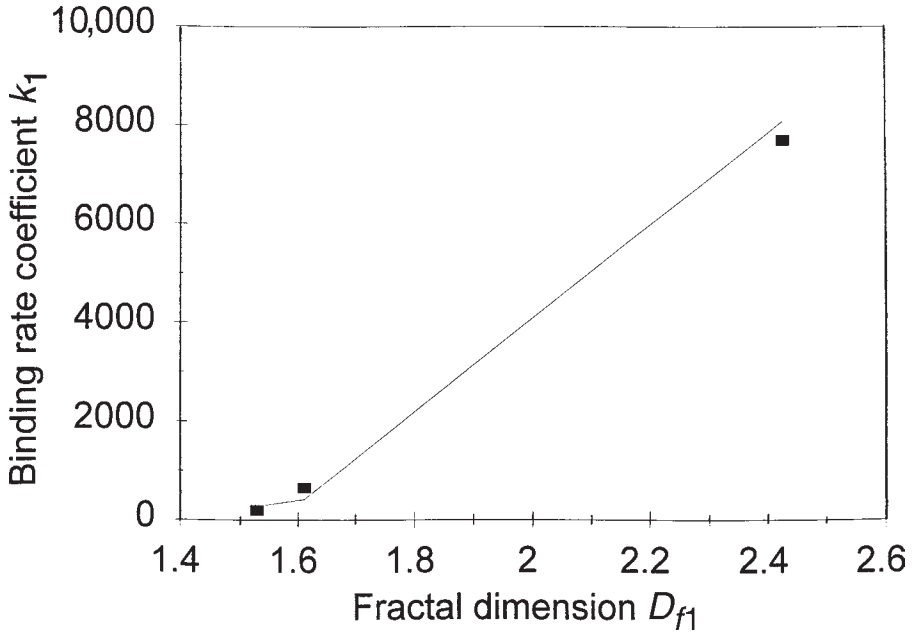

Fig. 6. Influence of the fractal dimension D_{f1} on the binding rate coefficient k_1.

diffusional limitations. This decrease in the diffusional limitations should then lead to an increase in the binding rate coefficient. Other suitable or more appropriate explanations to elucidate this effect are also possible.

Discussion

The fractal analysis of analyte-receptor binding kinetics we have presented provides examples of cases when a single-fractal analysis is applicable, a single- as well as a dual-fractal analysis is applicable, and a dual-fractal analysis is applicable. The fractal dimension D_f provides a quantitative measure of the degree of heterogeneity that exists on the surface. Also, a change from a single- to a dual-fractal analysis or the applicability of a dual-fractal analysis throughout a reaction indicates that there is a change in the binding mechanism as the reaction proceeds on the biosensor surface.

Predictive relationships developed for the binding rate coefficient as a function of a reactant concentration are of particular value because they provide an avenue through which one may manipulate the binding rate coefficient. These relationships have been developed for all of the three cases just mentioned. In each of these cases, the noninteger dependence of the binding rate coefficient on the reactant (or analyte) concentration or on the fractal dimension lends further support to the fractal nature of the system.

The fractal dimension is not a typical independent variable, such as analyte concentration, that may be directly manipulated. It is estimated from Eqs. 2a and 2b, and one may consider it as a "derived" variable. The

predictive relationship developed for the binding rate coefficient as a function of the fractal dimension is of considerable value because it directly links the binding rate coefficient to the degree of heterogeneity that exists on the surface, and it provides a means by which the binding rate coefficient may be manipulated by changing the degree of heterogeneity that exists on the surface. The binding rate coefficient k_1 is rather sensitive to D_{f1} or the degree of heterogeneity that exists on the biosensor surface. This may be noted by the high order of dependence (7.25). It is suggested that the fractal surface (roughness) leads to turbulence, which enhances mixing, decreases diffusional limitations, and leads to an increase in the binding rate coefficient *(50)*.

More studies are required to determine whether the binding rate coefficient is sensitive to the fractal dimension or the degree of heterogeneity that exists on the biosensor surface. If this is indeed so, experimentalists would be encouraged to pay more attention to the nature of the surface and how it may be manipulated to control the relevant parameters and biosensor performance in desired directions. Finally, in a more general sense, the treatment should also be applicable to nonbiosensor applications wherein further physical insights could be obtained.

References

1. Myszka, D. G., Morton, T. A., Doyle, M. L., and Chaiken, I. M. (1997), *Biophys. Chem.* **64,** 127–137.
2. Scheller, F. W., Hintsche, R., Pfeifer, D., Schubert, D., Reidel, K., and Kindevater, R. (1991), *Sens. Actuators* **4,** 197–206.
3. Pisarchick, M. L., Gesty, D., and Thompson, N. L. (1992), *Biophys. J.* **63,** 215–223.
4. Bluestein, B. I., Craig, M., Slovacek, R., Stundtner, L., Uricouli, C., Walziak, I., and Luderer, A. (1991), in *Biosensors with Fiberoptics*, Wise, D. and Wingard, L. B., Jr., eds., Humana, Clifton, NJ, pp. 181–223.
5. Eddowes, M. J. (1987/1988), *Biosensors* **3,** 1–15.
6. Place, J. F., Sutherland, R. M., Riley, A., and Mangan, C. (1991), in *Biosensors with Fiberoptics*, Wise, D. and Wingard, L. B., Jr., eds., Humana, Clifton, NJ, pp. 253–291.
7. Giaver, I. (1976), *J. Immunol.* **116,** 766–771.
8. Glaser, R. W. (1993), *Anal. Biochem.* **213,** 152–161.
9. Fischer, R. J., Fivash, M., Casas-Finet, J., Bladen, S., and McNitt, K. L. (1994), *Methods: Companion Methods Enzymol.* **6,** 121–133.
10. Stenberg, M., Stiblert, L., and Nygren, H. A. (1986), *J. Theor. Biol.* **120,** 129–142.
11. Nygren, H. A. and Stenberg, M. (1985), *J. Colloid Interface Sci.* **107,** 560–566.
12. Stenberg, M. and Nygren, H. A. (1982), *Anal. Biochem.* **127,** 183–192.
13. Morton, T. A., Myszka, D. G., and Chaiken, I. M. (1995), *Anal. Biochem.* **227,** 176–185.
14. Sjolander, S. and Urbaniczky, C. (1991), *Anal. Chem.* **63,** 2338–2345.
15. Sadana, A. and Sii, D. (1992), *J. Colloid Interface Sci.* **151(1),** 166–177.
16. Sadana, A. and Sii, D. (1992), *Biosens. Bioelectron.* **7,** 559–568.
17. Sadana, A. and Madagula, A. (1994), *Biosens. Bioelectron.* **9,** 45–55.
18. Sadana, A. and Beelaram, A. (1995), *Biosens. Bioelectron.* **10(3–4),** 301–316.
19. Christensen, L. L. H. (1997), *Anal. Biochem.* **249,** 153–164.
20. Matsuda, H. (1967), *J. Electroanal. Chem.* **179,** 107–117.
21. Elbicke, J. M., Morgan, D. M., and Weber, S. G. (1984), *Anal. Chem.* **56,** 978–985.
22. Edwards, P. R., Gill, A., Pollard-Knight, D. V., Hoare, M., Buckle, P. E., Lowe, P. A., and Leatherbarrow, R. J. (1995), *Anal. Biochem.* **231,** 210–217.
23. Chiu, N. H. L. and Christpoulos, T. K., (1996), *Anal. Chem.* **68,** 2304–2308.

24. Syvanen, A. C., Laaksonen, M., and Sonderlund, H. (1986), *Nucleic Acids Res.* **14(2),** 5037–5048.
25. Bier, F. F., Kleinjung, F., and Scheller, F. W. (1997), *Sens. Actuators* **38–39,** 78–82.
26. Nylander, C., Liedberg, B., and Lind, T. (1991), *Sens. Actuators* **3,** 79.
27. Bowles, M. R., Hall, D. R., Pond, S. M., and Winzor, D. J. (1997), *Anal. Biochem.* **244,** 133–143.
28. Schmitt, H. M., Brecht, A., Piehler, J., and Gauglitz, G. (1997), *Biosens. Bioelectron.* **12(8),** 809–816.
29. Kopelman, R. (1988), *Science* **241,** 1620–1626.
30. Pfeifer, P. and Obert, M. (1989), in *The Fractal Approach to Heterogeneous Chemistry: Surfaces, Colloids, Polymers*, Avnir, D., ed., J Wiley, New York, pp. 11–43.
31. Pajkossy, T. and Nyikos, L. (1989), *Electrochim. Acta* **34(2),** 171–177.
32. Markel, V. A., Muratov, L. S., Stockman, M. I., and George, T. F. (1991), *Phys. Rev. B* **43(10),** 8183–8195.
33. Gaillot, C., Larre, C., Caminade, A.-M., and Majoral, J.-P. (1997), *Science* **277,** 1981–1984.
34. Liebovitch, L. S. and Sullivan, J. M. (1987), *Biophys. J.* **52,** 979–988.
35. Liebovitch, L. S., Fischbarg, J., Koniarek, J. P., Todorova, I., and Wang, M. (1987), *Math. Biosci.* **84,** 37–68.
36. Li, H., Chen, S., and Zhao, H. (1990), *Biophys. J.* **58,** 1313–1320.
37. Dewey, T. G. and Bann, J. H. (1992), *Biophys. J.* **63,** 594–598.
38. Sorenson, C. M. and Roberts, G. C. (1997), *J. Colloid Interface Sci.* **186,** 447–456.
39. Sadana, A. (1997), *J. Colloid Interface Sci.* **190,** 232–240.
40. Milum, J. and Sadana, A. (1997), *J. Colloid Interface Sci.* **187,** 128–138.
41. Sadana, A. and Sutaria, M. (1997), *Biophys. Chem.* **65,** 29–44.
42. Sadana, A. (1998), *J. Colloid Interface Sci.* **198,** 164–178.
43. Sadana, A. and Madagula, A. (1993), *Biotechnol. Prog.* **9,** 259–266.
44. Di Cera, E. (1991), *J. Chem. Phys.* **95(2),** 5082–5086.
45. Anderson, J. (1993), Paper presented at NIH Panel Review Meeting, Case Western Reserve University, Cleveland, OH, July.
46. Sadana, A. (1995), *Biotechnol. Prog.* **11,** 50–57.
47. Havlin, S. (1989), in *The Fractal Approach to Heterogeneous Chemistry: Surfaces, Colloids, Polymers*, Avnir, D., ed., Wiley, New York, pp. 251–269.
48. Sigmaplot. (1993), *Scientific Graphing Software, User's Manual*, Jandel Scientific, San Rafael, CA.
49. Su, H., Chong, S., and Thompson, M. (1997), *Biosens. Bioelectron.* **12(3),** 161–173.
50. Martin, S. J., Granstaff, V. E., and Frye, G. C. (1991), *Anal. Chem.* **65,** 2910–2922.